

Article

A Control Method for Water Cannon of Unmanned Fireboats Considering Wind and Ship Motion Disturbances

Diju Gao ¹, Weixi Xie ^{1,*}, Chunteng Bao ¹, Bin Liu ² and Jiaxing Zhuang ²

¹ Key Laboratory of Transport Industry of Marine Technology and Control Engineering, Shanghai Maritime University, Shanghai 201306, China

² Shanghai Marine Equipment Research Institute, Shanghai 201203, China

* Correspondence: weixi_xie@163.com

Abstract: In order to realize accurate and fast firefighting at sea, a control method for water cannons of unmanned fireboats considering wind and ship motion disturbances is presented. This method combines information fusion, computer vision, and prediction technology based on neural network. Firstly, a prediction model of the jet trajectory of the fire water cannon considering the disturbances of constant horizontal wind is established, and the effective range of the water cannon's angles under the target working environment is obtained. Secondly, fusing the visual recognition information and predicted ship motion attitudes information, a double adaptive fuzzy controller is designed to compensate for the disturbances caused by the change in ship motion attitudes. Meanwhile, the online particle swarm optimization (PSO) is applied to fuzzy control to improve operational accuracy while enhancing the ability to adapt to environmental changes. The proposed control method was experimentally verified. As a result, the adaptive fuzzy controller based on the PSO can self-adjust the parameters to adapt to the changes in the working environment within 0.6 s, and the efficiency is improved by about 20%~50% compared with the traditional fuzzy control. The double adaptive fuzzy control can reach a stable and effective working state within 10 simulation steps, and the RMSE of the drop point error is only 3×10^{-3} m for 40 simulation steps after stabilization, which can effectively resist disturbances and improve efficiency and control accuracy. The control method can provide a practical reference for engineering applications of water cannon control of unmanned fireboats.



Citation: Gao, D.; Xie, W.; Bao, C.; Liu, B.; Zhuang, J. A Control Method for Water Cannon of Unmanned Fireboats Considering Wind and Ship Motion Disturbances. *J. Mar. Sci. Eng.* **2023**, *11*, 445. <https://doi.org/10.3390/jmse11020445>

Received: 1 January 2023

Revised: 22 January 2023

Accepted: 14 February 2023

Published: 17 February 2023



Copyright: © 2023 by the authors. Licensee MDPI, Basel, Switzerland. This article is an open access article distributed under the terms and conditions of the Creative Commons Attribution (CC BY) license (<https://creativecommons.org/licenses/by/4.0/>).

Keywords: water cannon; firefighting; ship motion; unmanned fireboat; double adaptive fuzzy control

1. Introduction

With the rapid development of the shipping industry, oil tankers and chemical tankers have become increasingly prominent in the water transportation industry. However, ship fires also occur frequently. For example, the Panamanian tanker Sanchi collided with a Hong Kong bulk carrier about 160 nautical miles east of the mouth of the Yangtze River in January 2018, resulting in the sinking of the Sanchi due to fire, and the leakage of partial condensate [1]. The bulk chemical vessel Hua Hong 18 was involved in a flash explosion at the Dongliang Mountain hazardous materials berthing area in the Yangtze River section of Wuhu City in September 2021, resulting in the death of three people [2]. Oil and chemicals are flammable and explosive, radioactive, etc. Once a fire occurs, it can easily cause enormous casualties, environmental pollution, economic losses, and adverse social impacts. Therefore, severe challenges are brought about by the rapid development of hazardous chemicals transportation to marine fire protection. While ensuring the safety of firefighters, fast and accurate firefighting and rescue work is the core goal of marine firefighting. Therefore, intelligent firefighting is an inevitable development trend of future marine firefighting and rescue. The water cannon is the actuator of the fireboat, and the gun head is adjusted according to the fire information detected by the fireboat for the sprayed

water to reach the expected position. However, wind and ship motion disturbances make the water cannon's control nonlinear and with strong coupling. These disturbances can lead to wasted firefighting resources, spreading flames, and can even endanger lives. Resisting wind and ship motion disturbances to improve the accuracy and responsiveness of the water cannon drop control is critical for unmanned fireboats.

Currently, there are two methods to control water cannons accurately: jet trajectory localization based on particle motion laws [3–5] and adjustment based on computer vision. The former method is used to analyze and simulate the influence factors of the jet according to the theory of physical particle kinematics and ballistics, and then estimate the jet's trajectory based on the parabola motion of the particle. However, factors such as air resistance are difficult to obtain precisely. As a result, it is difficult to locate the jet's trajectory by simple particle motion laws and mathematical calculations, so the control accuracy is not ideal. The computer-vision-based adjustment method can pick up the fire's location and the jet's drop point in the image. Calculating the deviation between the drop and the fire can help to determine whether the jet accurately hits the target. If it does not, the water cannon is adjusted according to the deviation to achieve closed-loop control. In recent years, this method has received increasing attention from scholars. Yongming et al. designed a fuzzy controller to perform closed-loop control of the horizontal and pitch angles of the water cannon based on computer vision recognition technology [6]. Jinsong et al. proposed an adaptive image threshold score method for image background segmentation and fire acquisition based on infrared vision, and designed a fuzzy controller for closed-loop control of water cannons by simulating firefighter operation patterns [7]. Jianshe et al. combined the localization method of jet trajectory with the adjustment method of computer vision to achieve closed-loop control of the water cannon [8]. In the research of this method, the fuzzy controller plays an important role. Fuzzy control is widely used in various fields due to its heuristic nature, simplicity, and effectiveness for linear and nonlinear systems [9–11]; however, it also has the prominent shortcoming of parameter sensitivity. In order to make up for this shortcoming, adaptive fuzzy control has been further developed. The main development directions of adaptive fuzzy control include fuzzy compound controller [12–14], optimization algorithm fuzzy control [15–18], neural network fuzzy control [19,20], multivariable fuzzy control [21,22], etc. Among them, with the vigorous development of metaheuristic intelligent optimization algorithms [23], the fuzzy control optimization algorithm shows great potential.

According to a lot of research, the computer-vision-based adjustment method is better than the particle-motion-based control method. However, the disturbances caused by wind and ship motion cannot be ignored in the marine fire protection application scenario, which is not considered in the current research. To this end, this paper proposes a control method for the water cannons of unmanned fireboats considering wind and ship motion disturbances. Firstly, we consider the disturbances of offshore operations and analyze the force on the jet microelement to obtain the jet trajectory model of the fire water cannon. The fourth-order Runge–Kutta numerical method is used to solve the initial value problem of ordinary differential equations to obtain the effective range of the water cannon's angles under the target working environment. Secondly, to improve the control method's timeliness, adaptive capability, and antidisturbance capability, a double adaptive fuzzy controller is designed based on improved fuzzy control using the linear particle swarm optimization (PSO). The controller realizes self-adjusting parameters to adapt to different working conditions and effectively resists wind and wave disturbances through the fusion of visual recognition information and predicted ship motion attitudes information.

This paper is organized as follows: Section 2 introduces the predictive model for water cannon jet trajectory considering disturbances. Section 3 investigates the effects of the ship's roll and pitch on the control of firefighting water cannons. In Section 4, the double adaptive fuzzy controller is introduced. Section 5 gives the simulation results and analysis. Section 6 concludes this paper.

2. A Predictive Model for Water Cannon Jet Trajectory Considering Disturbances

Constant Horizontal Wind Disturbance

Combined with the application scenario of offshore firefighting, the constant horizontal wind disturbance is considered, and the jet microelement of unit mass is taken as the research object. The jet is mainly affected by gravity, air resistance, and constant horizontal wind. Air resistance is generally considered proportional to the square of the jet velocity, which is opposite to and co-linear with the jet velocity. However, in the actual injection process, the jet's fragmentation phenomenon can deflect the air resistance direction by some angles. Constant horizontal wind not only produces disturbances in the direction of jet motion but is also a significant factor affecting the change in the horizontal angle of the jet. A schematic diagram of the force analysis of the jet microelement is shown in Figure 1.

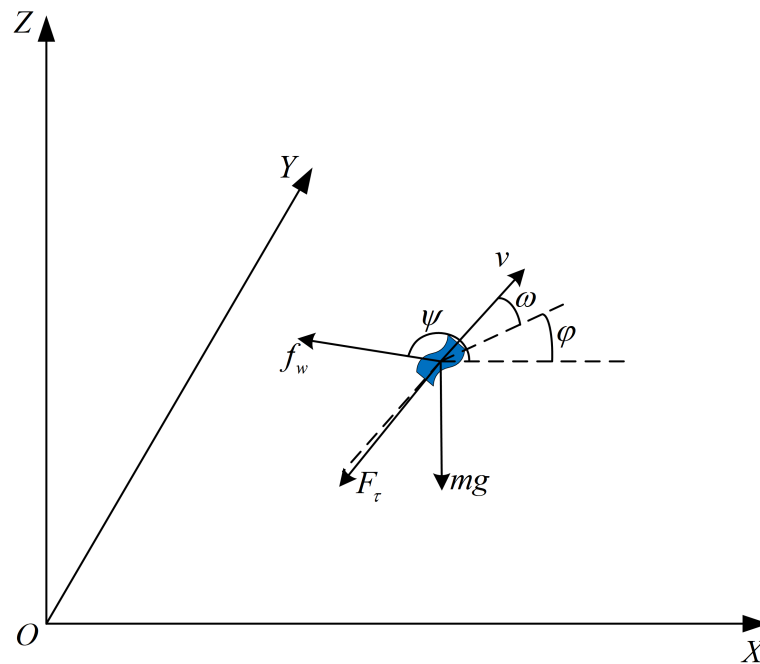


Figure 1. Schematic diagram of the force analysis of a jet microelement.

Let \vec{v} be the velocity vector in the direction of motion of the jet microelement, v be the module of \vec{v} , and \vec{i} be the unit vector in the direction of \vec{v} . \vec{v} is determined by:

$$\vec{v} = v\vec{i} \tag{1}$$

Differentiating both ends of (1) with respect to time gives:

$$\frac{d\vec{v}}{dt} = \frac{dv}{dt}\vec{i} + \frac{d\vec{i}}{dt}v \tag{2}$$

Let \vec{j} be the unit vector in the normal direction perpendicular to \vec{v} and parallel to the $X_0O_0Y_0$, and let ω be the angle between \vec{v} and $X_0O_0Y_0$.

$$\frac{d\vec{i}}{dt} = \frac{d\vec{i}}{d\omega} \frac{d\omega}{dt} = \frac{d\vec{i}}{d\omega} \vec{j} \tag{3}$$

Thus, (2) can be transformed into:

$$\frac{d\vec{v}}{dt} = \frac{dv}{dt}\vec{i} + v \frac{d\omega}{dt} \vec{j} \tag{4}$$

From (4), the acceleration in the direction of jet motion is equal to the vector sum of the acceleration in the tangential and normal directions of the jet trajectory. Multiplying both ends of (4) by the mass of the jet microelement obtains:

$$m \frac{d\vec{v}}{dt} = m \frac{dv}{dt} \vec{i} + mv \frac{d\vec{\omega}}{dt} \vec{j} \tag{5}$$

Projecting (5) in the direction of \vec{i} and \vec{j} for specific analysis, the changes in v and ω are produced by the combined effect of gravity mg , air resistance F_τ , and wind disturbance f_w . The effect of F_τ on angular acceleration is expressed as a factor k .

$$m \frac{dv}{dt} = f_w \cos(\psi - \varphi) \sin\omega - F_\tau - mg \sin\omega \tag{6}$$

$$mv \frac{d\omega}{dt} = -k(f_w \cos(\psi - \varphi) \sin\omega + mg \sin\omega) \tag{7}$$

where ω is the angle between the projection point of the jet microelement on $X_0O_0Y_0$ and the positive direction of $\vec{O_0X_0}$, and φ is the angle between the horizontal wind direction and the positive direction of $\vec{O_0X_0}$.

The jet microelement's position constantly changes in the coordinate system. The change of x and y coordinates is produced by v and f_w together, and the change of z coordinates is caused by v only.

$$\frac{dx}{dt} = v \cos\omega \cos\varphi - f_w \sin(\psi - \varphi) \sin\varphi \tag{8}$$

$$\frac{dy}{dt} = v \cos\omega \sin\varphi + f_w \sin(\psi - \varphi) \cos\varphi \tag{9}$$

$$\frac{dz}{dt} = v \sin\omega \tag{10}$$

In addition, microelement's φ also changes continuously due to the disturbances of the constant horizontal wind, and the change in φ is mainly caused by f_w , which can be expressed as:

$$\frac{d\varphi}{dt} = \arctan\left(\frac{y + dy}{x + dx}\right) - \arctan\left(\frac{y}{x}\right) \tag{11}$$

The trajectory of the jet can be divided by the highest point of the trajectory. It is divided into a rising section and a falling section. By analyzing the actual trajectory of the jet, it is found that the rate of change of the jet velocity direction, i.e., the angular acceleration, is significantly different in the two sections.

The set of differential equations for the prediction model of the jet trajectory of a water cannon under consideration of disturbances is expressed as:

$$\begin{cases} \frac{dv}{dt} = \frac{f_w \cos(\psi - \varphi) \cos\omega - F_\tau}{m} - g \sin\omega \\ \frac{d\omega}{dt} = -k \left(\frac{f_w \cos(\psi - \varphi) \sin\omega}{m} + \frac{g \cos\omega}{v} \right) \\ \frac{d\varphi}{dt} = \arctan\left(\frac{y + dy}{x + dx}\right) - \arctan\left(\frac{y}{x}\right) \\ \frac{dx}{dt} = v \cos\omega \cos\varphi - f_w \sin(\psi - \varphi) \sin\varphi \\ \frac{dy}{dt} = v \cos\omega \sin\varphi + f_w \sin(\psi - \varphi) \cos\varphi \\ \frac{dz}{dt} = v \sin\omega \end{cases} \tag{12}$$

where k is the angular acceleration correction factor, which is k_1 in the ascent section and k_2 in the rise section.

The wind-pressure relationship derived from Bernoulli's equation gives the dynamic pressure of the wind as [24]

$$wp = 0.5 \rho_{air} v_w^2 \tag{13}$$

where ρ_{air} is the air density and v_w is the wind speed. Since the relationship between air density ρ_{air} and air weight γ can be expressed as g through gravitational acceleration $\rho_{air} = \gamma/g$, (13) can be expressed as:

$$wp = 0.5\gamma \frac{v_w^2}{g} \tag{14}$$

(14) is the standard wind-pressure equation in the standard state (air pressure of 1013 hPa and temperature of 15 °C), air gravity $\gamma = 0.01225 \text{ n/m}^3$ and gravitational acceleration $g = 9.8 \text{ m/s}^2$ at a latitude of 45°, and thus the wind-pressure is

$$wp = \frac{v_w^2}{1600} \tag{15}$$

(15) is used in this paper for estimating wind pressure from wind speed. Let the side area of a jet microelement perpendicular to the direction of \vec{j} be $S_{Lateral}$, and f_w can be expressed as:

$$f_w = 100wpS_{Lateral}g \tag{16}$$

According to the principle of external ballistics, the jet microelement moving in the air is approximated as a projectile with velocity below Mach 1, so the air resistance to the jet microelement can be expressed as [25]:

$$F_\tau = 0.5\rho_{water}v^2S_M C_x \tag{17}$$

In (17), ρ_{water} is the density of water, S_M is the cross-sectional area of the jet, and C_x is the air resistance coefficient.

Air resistance is generally made up of three parts: friction, vortex, and wave resistance. From practical experience, when the object's flight speed is less than 0.6 Mach, the surge phenomenon will not produce, that is, it will not produce wave resistance. Thus, for the friction and vortex resistance for the jet in motion by the main components of air resistance, in this case, the air resistance coefficient C_x available Reynolds number R_e is defined as:

$$C_x = \frac{0.072}{R_e^{0.2}} + 0.108R_e^{0.1} \tag{18}$$

$$R_e = \frac{\rho_{water}vd}{\mu} \tag{19}$$

In (19), v and d are the velocity of the jet and the equivalent diameter of the jet, and μ is the dynamic viscosity coefficient of water.

In addition, according to the characteristics of the jet trajectory of the water cannon, it is known that the length of the rising section in the horizontal direction is greater than the height in the vertical direction, and the height of the vertical direction of the falling section is greater than the length in the horizontal direction. Thus, the calculation for the cross-sectional area of the two stages is also different.

The cross-sectional area of the rising section is defined as:

$$S_M = A_a(1 + a\ln(1 + \sqrt{x^2 + y^2})) \tag{20}$$

where A_a is the cross-sectional area of the nozzle, and a is the coefficient of variation of the cross-sectional area of the rising section.

The cross-sectional area of the falling section is defined as:

$$S_M = A_b(1 + b\ln(1 + z_0 - z)) \tag{21}$$

where A_b is the cross-sectional area at the highest point of the jet, b is the coefficient of variation of the cross-sectional area of the falling section, and z_0 is the height at the highest point of the jet.

All the above derivation processes and related studies in the later sections are based on the following assumptions and descriptions.

- Two kinds of coordinate systems are used: one is called the Earth coordinate system $O_0 - X_0Y_0Z_0$, the origin of which is located on the stationary water surface, $\vec{O_0X_0}$ points to due north, $\vec{O_0Y_0}$ points to due east, and $\vec{O_0Z_0}$ points to the center of the Earth, which is used to describe the position of firefighting water cannon and jet microelement. Another is called the attached coordinate system $O - XYZ$, the origin of which is located at the center of gravity of the ship, \vec{OX} points to the bow, \vec{OY} points to the starboard side, and \vec{OZ} points to the bottom of the ship, which is used to describe the motion attitude of the ship.
- Working environment: Class III sea state, Class III wind. Wind speed is 3.4~5.4 m/s, wind pressure is 0.72~1.82 kg/m², and wave height range is 0.5~1.25 m.
- Parameter values: The values of air density, water density, and dynamic viscosity coefficient of water are used in the standard state, which is 1.29 kg/m³, 999.1 kg/m³, and 0.001144 Pa.S, respectively. Gravitational acceleration is chosen to be 9.8 m/s² at latitude 45°. Furthermore, the operational process occurs near the surface, which can be assumed to remain constant, and gravity does not change.

3. Ship Motion Disturbance

In addition to the disturbances of constant horizontal wind, the variation of motion attitudes of unmanned fireboats can also lead to errors in water cannon control. Therefore, this paper investigates the effects of ship’s roll and pitch on the control of firefighting water cannons to counteract the disturbances caused by them. Table 1 defines the ship motion attitudes and water cannon’s control quantities, where the maximum ship leaning left is -180° , the maximum ship leaning back is -90° , and the horizontal angle when the water cannon is pointing at the transom is 0° .

Table 1. Definition of ship motion attitudes and control quantities of water cannon.

Variable Name	Value
Ship’s roll angle (α_{roll})	$[-180^\circ, 180^\circ]$
Ship’s pitch angle (α_{pitch})	$[-90^\circ, 90^\circ]$
Cannon’s pitch angle (θ)	$[18^\circ, 80^\circ]$
Cannon’s horizontal angle (β)	$[0^\circ, 180^\circ]$

Under the condition of ignoring the coupled motion of the ship’s roll and pitch, the perturbation of the pitch angle θ of the water cannon is mainly due to roll. When the ship’s roll attitudes changes, the pitch angle of the water cannon relative to the horizontal plane will also change accordingly, and the disturbances amount $\theta_d(t + 1)$ of the pitch angle at the next moment can be expressed by the difference between the roll angle at the next moment with the current moment. The specific calculation is expressed as:

$$\theta_d(t + 1) = \alpha_{roll}(t + 1) - \alpha_{roll}(t) \tag{22}$$

where $\alpha_{roll}(t)$ is the current moment of roll angle and $\alpha_{roll}(t + 1)$ is the next moment of roll angle.

The disturbances of the horizontal angle β of the water cannon are mainly due to pitch. When the ship’s pitch attitudes changes, the water cannon will be displaced in the X-axis direction producing different desired horizontal angles. In this paper, the change of ship attitudes is microamplitude, so the degree of disturbances of the constant horizontal wind disturbances to the jet is the same before and after the desired horizontal angle change.

Under the condition of neglecting the effect of wind on the jet, the disturbance value of the next horizontal angle can be expressed as the difference between the expected horizontal angle of the water cannon before and after the disturbance. The specific calculation is expressed as:

$$\begin{cases} \Delta x = h\sin\alpha_{pitch}(t+1) - h\sin\alpha_{pitch}(t) \\ \delta(t+1) = \arctan(SR\sin\delta(t), \Delta x + SR\cos\delta(t)) \\ \beta_d(t+1) = \delta(t+1) - \delta(t) \end{cases} \quad (23)$$

wherein Δx is the X-axis displacement due to the change in longitudinal sway attitude, and h is the vertical distance between the water cannon and the horizontal plane where the ship's center of gravity is located. $\alpha_{pitch}(t)$ and $\alpha_{pitch}(t+1)$ are the pitch angles of the ship at the current and next moment, respectively. SR is the straight-line distance between the water cannon and the target point at the current moment. $\delta(t)$ and $\delta(t+1)$ are approximate and desired horizontal angles of the water cannon at the current and next moments, respectively.

4. Double Adaptive Fuzzy Control

Fuzzy control is the most commonly used method for water cannons. However, the working environment of offshore firefighting is complex; wind and ship motion change continuously and frequently. Fuzzy control is parameter-sensitive and poorly adaptable to the environment, which cannot meet the needs of marine fire water cannon control. Therefore, based on optimization algorithm fuzzy control [15], PSO is used to improve the fuzzy control and adjust the parameters of the fuzzy controller adaptively, and then it changes the interval range of the fuzzy controller.

4.1. Online Adaptive Module

The total number of PSO particles was set as 1, and the result of two successive attitude adjustments of the water cannon was used as the evaluation basis of the current particles (the current scale factor and quantitative factor of the fuzzy controller). After continuous iteration of the PSO, the controller parameters were adjusted adaptively to change the interval range of the controller. In addition, during the experiment, due to the composition characteristics of the fitness function designed in this paper, the adjustment speed of the horizontal deflection angle was generally faster than that of the pitch angle, resulting in an overadjustment phenomenon. Therefore, the weight coefficient was added to the fitness function. After several simulations, the effect of 1:4 was better, and the fitness function is shown in (24).

$$Fitness = \frac{|\Delta SR|}{|\Delta SR| + |\Delta\delta|} + 4 \frac{|\Delta\delta|}{|\Delta SR| + |\Delta\delta|} \quad (24)$$

Let SR_{jet} and SR_{tar} be the distance between the jet drop point and the target point to the water cannon, respectively, and \vec{p} be the negative direction of \vec{OX} . Then, in (24), $\Delta SR = SR_{jet} - SR_{tar}$, $\Delta\delta = \angle(SR_{jet}, \vec{p}) - \angle(SR_{tar}, \vec{p})$.

4.2. Double Fuzzy Controller Design

In order to resist the error of firefighting operation caused by ship motion, this paper adds the adaptive fuzzy controller II to the adaptive fuzzy control system based on visual recognition. The controller II provides the compensation value for water cannon adjustment, which is added to the primary adjustment value obtained from the controller I as the actual value of angles adjustment of the water cannon, thus effectively resisting ship motion disturbances. A block diagram of the water cannon control system of the unmanned fireboat considering wind and ship motion disturbances is shown in Figure 2.

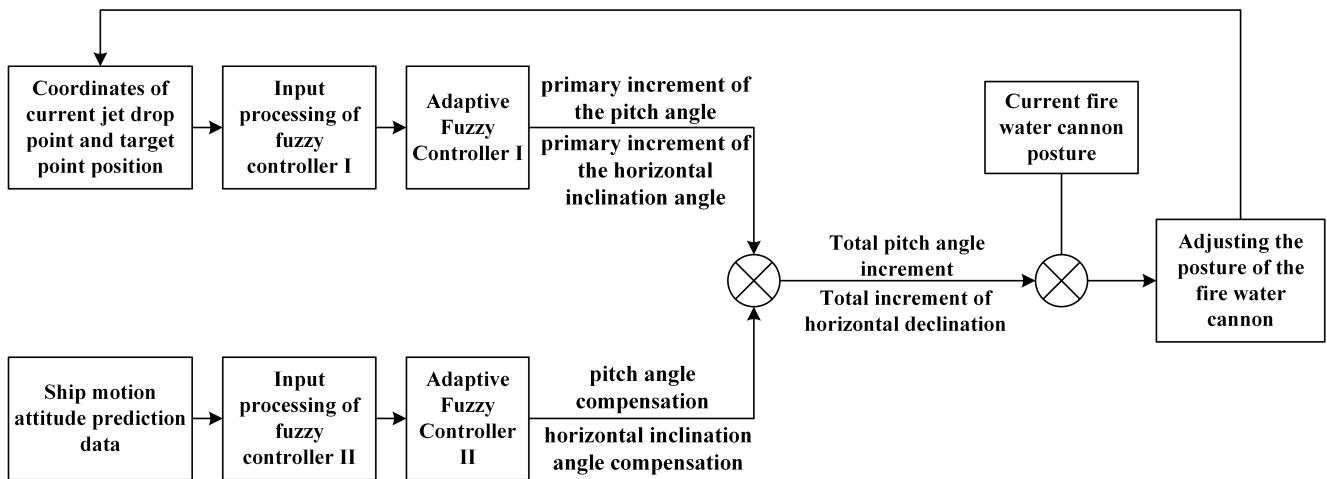


Figure 2. Block diagram of the water cannon control system of the unmanned fireboat considering wind and ship motion disturbances.

For the adaptive fuzzy controller I, primary increments of the pitch and horizontal angles $\Delta\theta_1$ and $\Delta\beta_1$ are output variables; ΔSR and its rate of change $d\Delta SR$, $\Delta\delta$ and its rate of change $d\Delta\delta$ are the input variables. For the adaptive fuzzy controller II, compensation adjustment values $\Delta\theta_2$ and $\Delta\beta_2$ for the water cannon’s pitch and horizontal angles are the output variables; water cannon attitudes disturbances $\theta_d(t + 1)$ and $\beta_d(t + 1)$, and their rates of change $d\theta_d$ and $d\beta_d$ are the input variables.

The fuzzy control affiliation function is selected as an isosceles triangle, as shown in Figure 3. When the number of fuzzy sets is seven, the fuzzy controller has good dynamic and static performance, more vital anti-interference ability, and is easy to implement [26]. Therefore, input and output variables are divided into seven fuzzy sets: NB, NM, NS, ZE, PS, PM, and PB, which correspond to negative large, negative medium, negative small, zero, positive small, positive medium, and positive large, respectively.

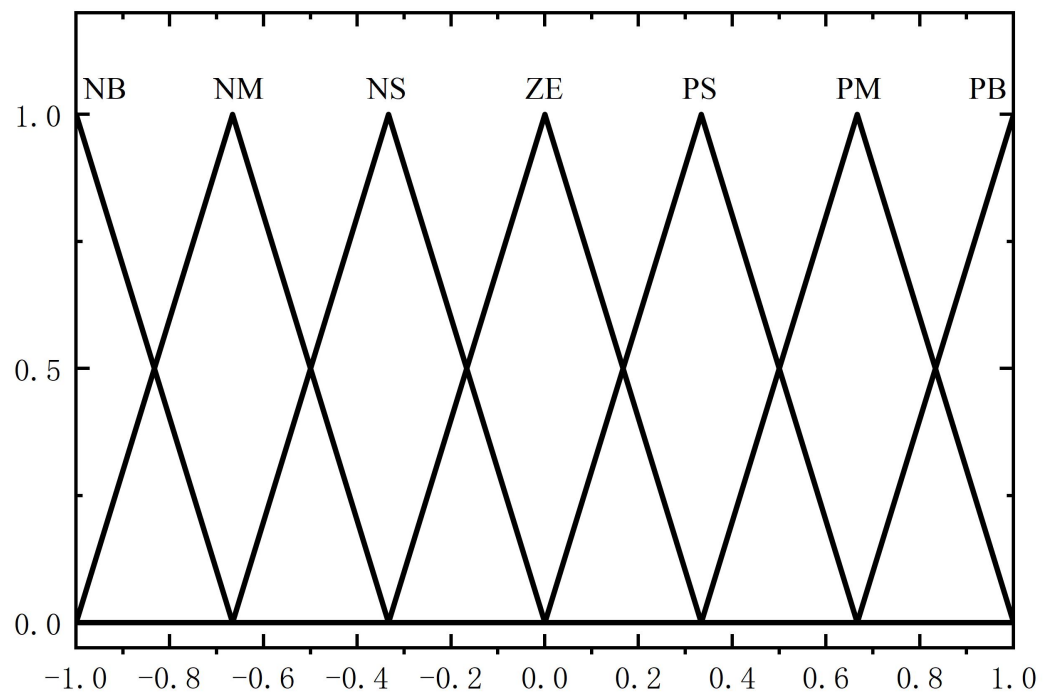


Figure 3. Fuzzy control affiliation function.

Take fuzzy controller II as an example to design fuzzy rules with reference to firefighters' experience adjusting horizontal and pitch angle. When the pitch angle disturbances $\theta_d(t + 1)$ are significant, and $d\theta_d$ is opposite to $\theta_d(t + 1)$, the pitch angle compensation value should be significant. When the horizontal angle disturbances $\beta_d(t + 1)$ are large, and $d\beta_d$ is opposite to $\beta_d(t + 1)$, the horizontal angle compensation value should be significant. The same rule applies to the controller I, and the fuzzy rule design is shown in Tables 2 and 3.

In adaptive fuzzy controllers I and II, Mamdani-type fuzzy inference method is used for decision making, and the center of gravity method is used for defuzzification.

Table 2. Fuzzy rules for $\Delta\theta_1$ and $\Delta\theta_2$.

$\Delta SR/\theta_d(t + 1)$	$d\Delta SR/d\theta_d$						
	NB	NM	NS	ZE	PS	PM	PB
NB	PB	PB	PM	PM	PS	PS	ZE
NM	PB	PM	PM	PS	PS	ZE	ZE
NS	PM	PM	PS	PS	ZE	ZE	ZE
ZE	PS	PS	ZE	ZE	ZE	NS	NS
PS	ZE	ZE	ZE	NS	NS	NM	NM
PM	ZE	ZE	NS	NM	NM	NM	NB
PB	ZE	NS	NS	NM	NM	NB	NB

Table 3. Fuzzy rules for $\Delta\beta_1$ and $\Delta\beta_2$.

$\Delta\delta/\beta_d(t + 1)$	$d\Delta\delta/d\beta_d$						
	NB	NM	NS	ZE	PS	PM	PB
NB	PB	PB	PM	PM	PS	PS	ZE
NM	PB	PM	PM	PS	PS	ZE	ZE
NS	PM	PM	PS	PS	ZE	ZE	ZE
ZE	PS	PS	ZE	ZE	ZE	NS	NS
PS	ZE	ZE	ZE	NS	NS	NM	NM
PM	ZE	ZE	NS	NM	NM	NM	NB
PB	ZE	NS	NS	NM	NM	NB	NB

5. Simulation and Analysis of Results

This paper assumes that the visual recognition information is all in existing and accurate conditions. In the simulation experiments, the position of the fire is constant as (60, 20, 0) in the Earth coordinate system, and the jet trajectory model calculates the position of the jet drop point.

The model was established by Matlab/Simulink. Table 4 shows the parameters of the fireboat, and the water cannon was mounted on the starboard side of the fireboat in the middle position. The coefficients a , b , k_1 , and k_2 in the jet trajectory prediction model were fitted using the values from [4] in Figure 4. The ship motion attitudes data in the simulation model were from [27] in Figure 5. The shipping speed was 0 kn, and the wind speed in the operating environment was 5.4 m/s. The wind angle was 45°. The cannon's initial pitch and horizontal angle were set to 30° and 0°, and the initial ship motion attitudes were set to $\alpha_{roll} = 0.65^\circ$ and $\alpha_{pitch} = -0.53^\circ$.

Table 4. Parameters of the fireboat.

Name	Parameter	Value
Ship	Overall length	35.00 m
	Length between columns	32.40 m
	Length of waterline	33.78 m
	Profile width	7.00 m
	Depth	3.20 m
	Design draft	2.10 m
	Crew	12 persons
	Sailing area	Inland river B class
	Speed	13.0 kn
Water cannon	Operating pressure	689.5 kPa
	Rated flow	94.625 L/s
	Equivalent diameter	57.15 mm
	Height of cannon head from the ground	0.61 m
	Muzzle initial velocity	36.89 m/s

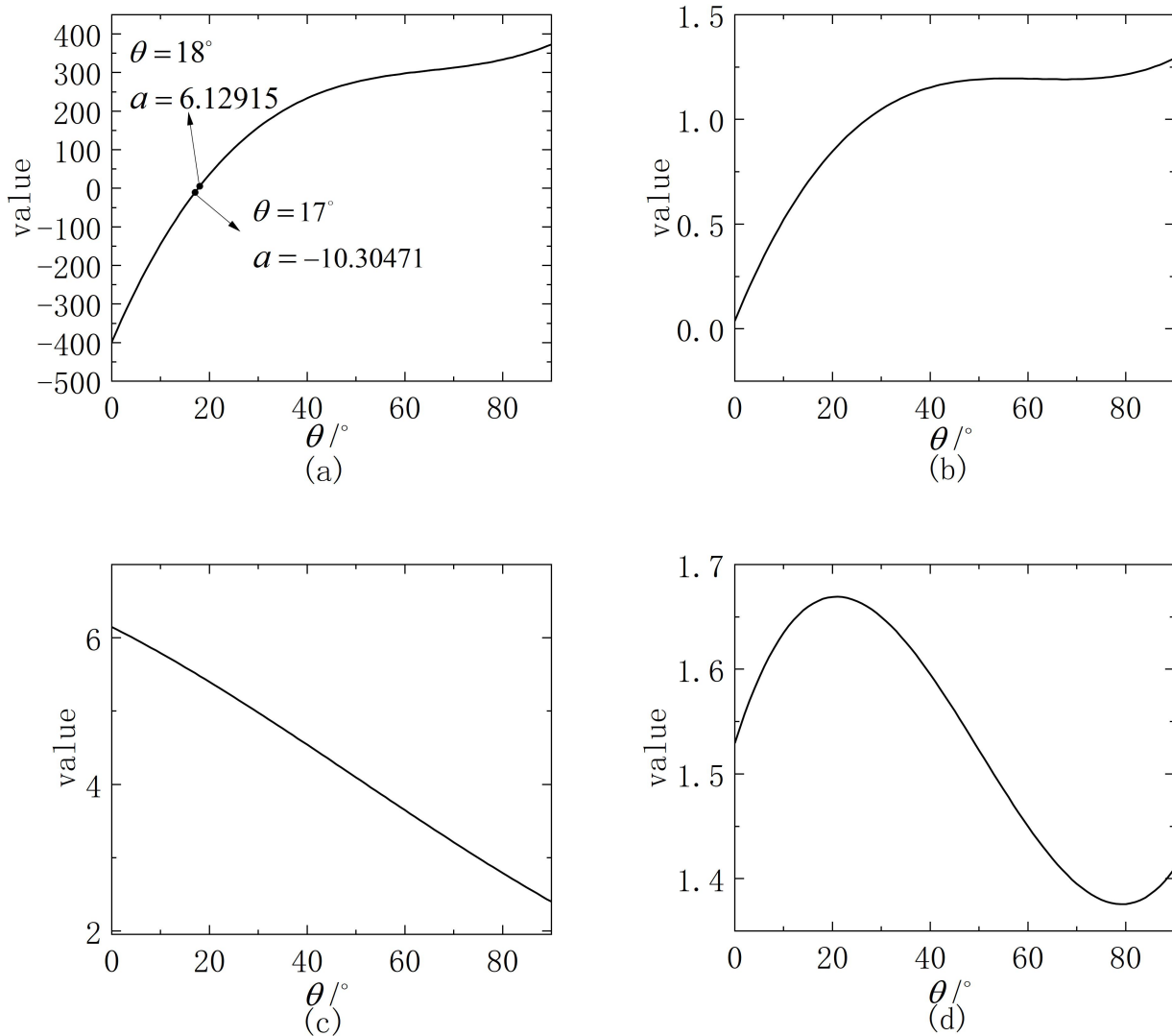


Figure 4. Jet trajectory prediction model coefficients: (a) coefficient of variation of the cross-sectional area of the rising section; (b) coefficient of variation of the cross-sectional area of the falling section; (c) angular acceleration correction factor in the ascent section; (d) angular acceleration correction factor in the rise section.

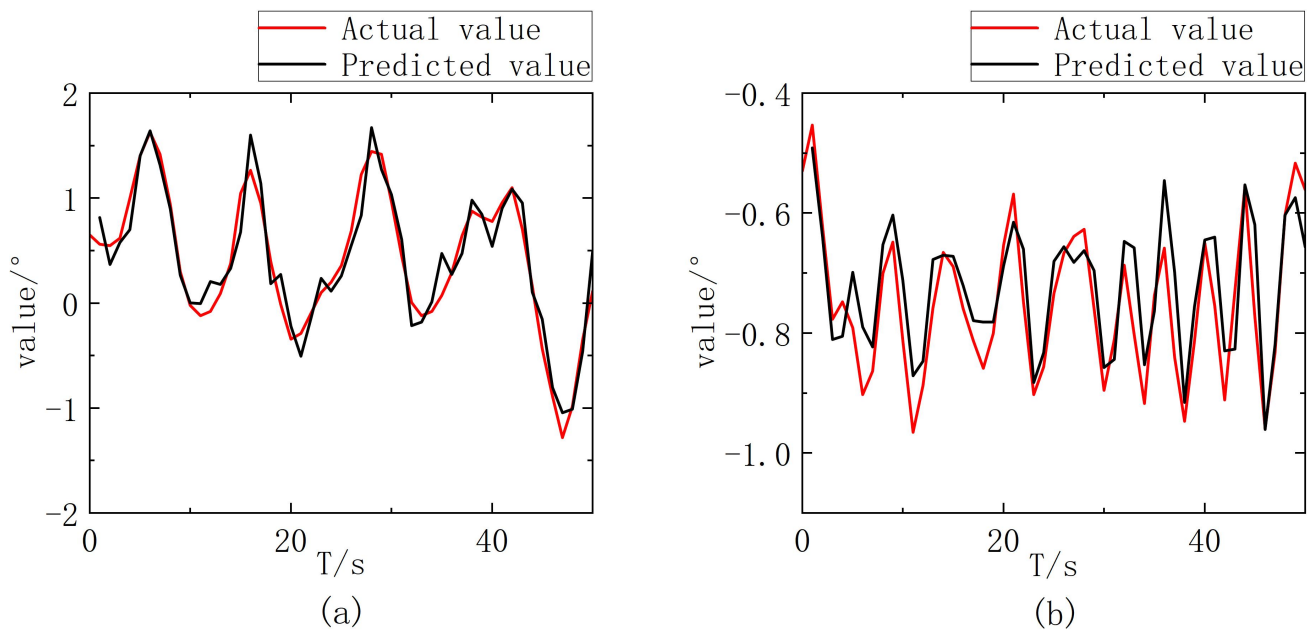


Figure 5. Ship motion attitudes: (a) ship’s roll angle; (b) ship’s pitch angle.

Then, as the cannon’s jet is elliptical when they land and cover a certain area, the drop point error is defined as an effective working state when it is less than 5×10^{-2} m, and (25) is used as the working efficiency calculation equation.

$$E = \frac{1}{t} \tag{25}$$

wherein t is the time required from the start of work to stable in the effective working state. The greater the value of efficiency E , the higher the efficiency of the current system. The size of the efficiency improvement can be calculated by:

$$E_{promotion} = \frac{E_{new} - E_{old}}{E_{old}} \times 100\% \tag{26}$$

In (26), E_{new} is the efficiency of the control method designed in this paper, and E_{old} is the efficiency of the control method used for comparison.

5.1. Simulation for Predicting the Jets Trajectory of a Water Cannon Considering Disturbances

It can be seen from Figure 4 that the obtained model correction coefficient a is invalid negative at $\theta \leq 17^\circ$ due to the insufficient number of experiments in the [6]. To verify the validity of the model and to determine the valid working interval, the model was established by Matlab/Simulink. Simulation results are shown in Figure 6. Multiple jet trajectory simulations were performed at different (θ, β, ψ) values, in which θ was set as $[18^\circ, 90^\circ]$ (step = 1°), β was set to 0° , and ψ was set as $[0^\circ, 360^\circ]$ (step = 2°); each curve on the graph corresponds to a pitch angle. As shown in Figure 6, when θ is in the range of 18° – 86° , the constant horizontal wind has little influence on the range. When θ exceeds 86° , the jet stays in the air for too long, and its direction will be out of control under the continuous action of the wind. In order to find the effective range of the water cannon’s angles, θ and $\psi - \beta$ were set to $[80^\circ, 90^\circ]$ and 131° , respectively, when simulating the 3D jet trajectory of the water cannon, and the results obtained are shown in Figure 7.

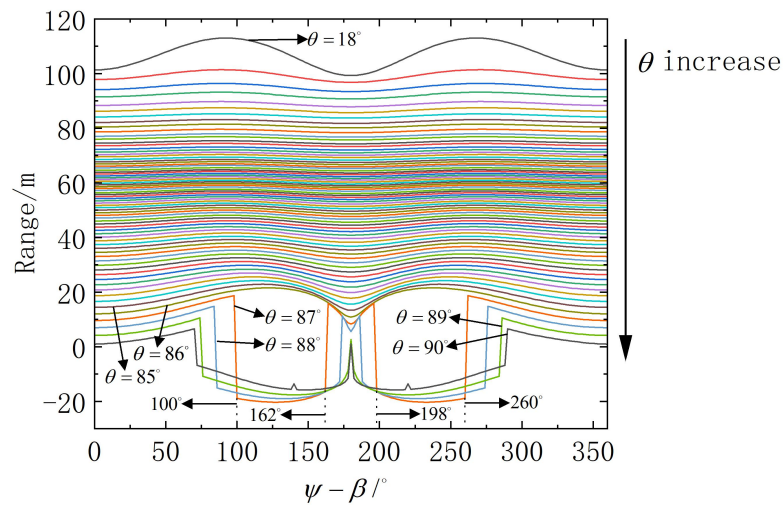


Figure 6. Simulation results of the range of a water cannon under constant horizontal wind disturbances.

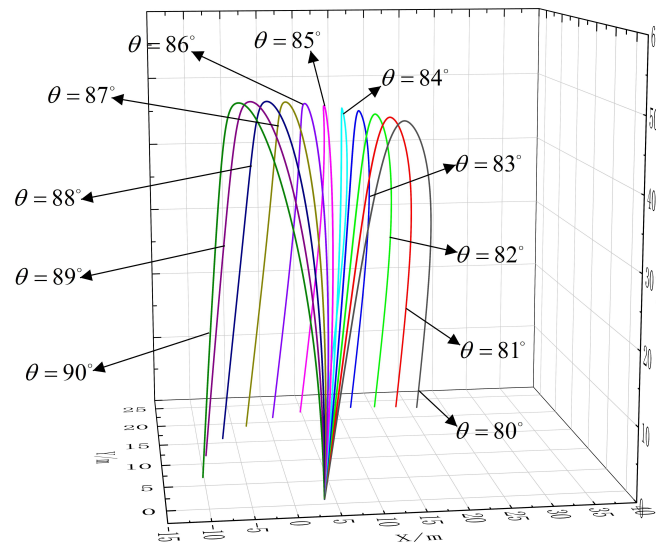


Figure 7. Simulation of the 3D jet trajectory of a water cannon under constant horizontal wind disturbances.

As shown in Figure 6, the effect of constant horizontal wind on the range of the water cannon is symmetrical along 180° in the range of $\psi - \beta = [0^\circ, 360^\circ]$. The overall effect is not significant due to the low level of the sea state, but at $\theta = [87^\circ, 89^\circ]$, there is a negative range. As shown in Figure 7, when θ is greater than 84° , it will lead to the jet staying in the air for too long. The horizontal velocity of the jet will gradually decrease until it is opposite to the initial direction. Eventually, the jet will fall inside the hull, or even on the other side, without practical operation.

In order to prevent the unmanned fireboat from falling into an ineffective working state in the current working environment, the effective range of θ can be limited to $[18^\circ, 80^\circ]$. At this time, when $\psi - \beta$ is any value of $[0^\circ, 360^\circ]$ it will not affect the operation, then the effective range of the β can be constrained to $[0^\circ, 180^\circ]$. At this time, the effective range of the firefighting water cannon is $[23.79 \text{ m}, 113.05 \text{ m}]$.

5.2. Simulation for Adaptive Fuzzy Control Method

In order to verify the adaptive capability of the controller designed in this paper, simulation comparison tests were conducted, and the results are shown in Table 5 and

Figure 8. Among them, the parameters of the nonadaptive fuzzy controller are shown in Table 6, which comes from [6]. The parameters of the adaptive fuzzy controller are shown in Table 7.

Table 5. Parameters of adaptive fuzzy controller based on PSO optimization.

Controller Parameter	Stable Value
k_{e1}	0.0225
$k_{\dot{e}1}$	0.01
k_{e2}	0.5508
$k_{\dot{e}2}$	0.1203
k_{u1}	0.5229
k_{u2}	1.1164

Table 6. Parameters of the nonadaptive fuzzy controller [6].

Controller Parameter	Value
k_{e1}	0.02
$k_{\dot{e}1}$	0.005
k_{e2}	0.5
$k_{\dot{e}2}$	0.2
k_{u1}	0.02
k_{u2}	0.1

Table 7. Parameters of the adaptive fuzzy controller (this paper).

Controller Parameter	Population Range	Speed Range	Initial Value
k_{e1}	0.01~0.03	-0.0005~0.0005	0.02
$k_{\dot{e}1}$	0.001~0.01	-0.001~0.001	0.005
k_{e2}	0.1~1	-0.005~0.005	0.5
$k_{\dot{e}2}$	0.1~0.3	-0.002~0.002	0.2
k_{u1}	0.01~1	-0.1~0.1	0.02
k_{u2}	0.1~1.5	-0.1~0.1	0.1

Table 5 shows the optimization results of controller parameters obtained through online particle swarm optimization algorithm self-adjustment. The drop point control error of the nonadaptive fuzzy controller (parameters are set as in Table 6) considering constant horizontal wind disturbances is shown in Figure 8a. Figure 8b shows the drop point control error of the nonadaptive fuzzy controller (parameters are set as in Table 6) without considering wind disturbances in [6]. Figure 8c shows that when environmental factors such as wind speed vary, the drop point control error of the adaptive fuzzy controller (parameters are set as in Table 7) considers wind disturbances. Figure 8d shows the drop point control error of the nonadaptive fuzzy controller considering wind disturbances when the parameters in Table 5 are adopted.

Figure 8a,b show that the nonadaptive fuzzy controller cannot maintain the same response speed and control accuracy in different operating environments. From Figure 8c, it can be seen that when the wind speed or other environmental factors change, the adaptive fuzzy controller adjusts its parameters by online PSO and can enter the state of stable and effective operation within 0.6 s. Compared with 0.72 s in Figure 8b, a 20% improvement in efficiency is obtained by (26). It can be seen from Figure 8d that the adaptive fuzzy controller can obtain a set of controller parameters at the end of the simulation, and, using this parameter for nonadaptive fuzzy control simulation, can enter the state of stable and effective operation within 0.48 s, which is 50% more efficient compared to Figure 8b. It shows that the adaptive fuzzy controller in this paper can dispense with the tedious and complicated parameter experiments, and also makes the system work in a better state by adaptive adjustment.

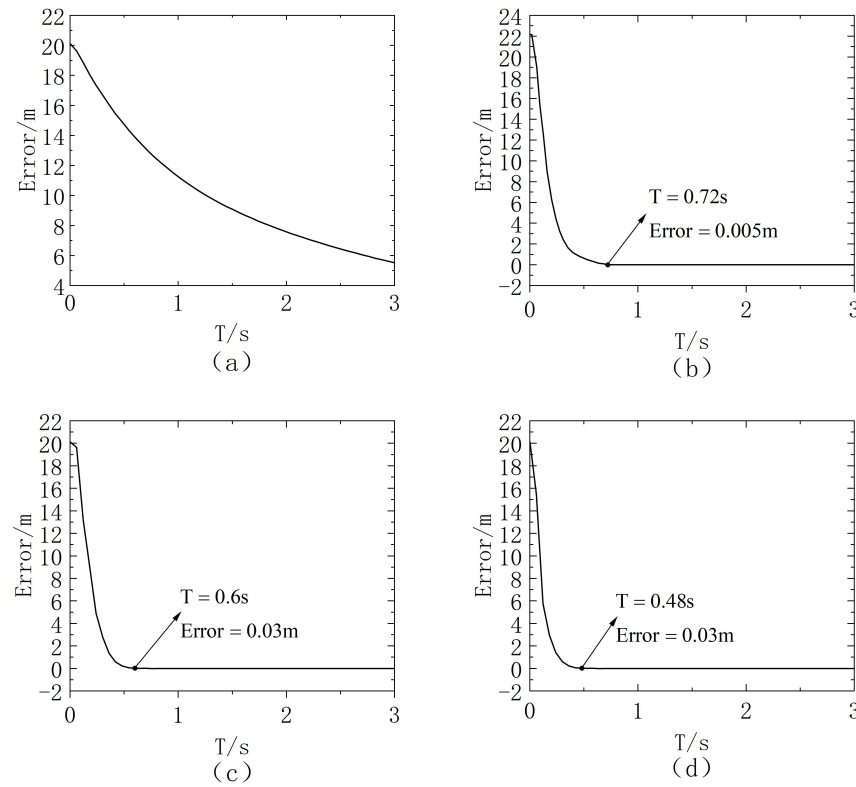


Figure 8. Drop point control error: (a) based on nonadaptive fuzzy controller considering constant horizontal wind disturbances; (b) based on nonadaptive fuzzy controller without considering wind disturbances; (c) based on adaptive fuzzy controller considering wind disturbances; (d) based on nonadaptive fuzzy controller considering wind disturbances.

5.3. Simulation for Double Adaptive Fuzzy Control

The strategy in Section 3 was used to quantify the effect of the ship motion attitudes in Figure 5 on firefighting operations. Simulation experiments were conducted based on the obtained disturbances values to verify the superiority of the double adaptive fuzzy control system in this paper. Parameters of the double adaptive fuzzy controller are shown in Table 8. The errors of drop point control by double adaptive fuzzy control are shown in Figure 9. The comparative results of the firefighting performance by calculating the RMSE of the drop point error are shown in Table 9.

Table 8. Parameters of the double adaptive fuzzy controller.

Variable	Controller Parameter	Population Range	Speed Range	Initial Value
ΔSR	k_{e1}	0.01~0.03	-0.0005~0.0005	0.02
$d\Delta SR$	k_{e1}	0.001~0.01	-0.001~0.001	0.005
$\Delta\beta$	k_{e2}	0.1~1	-0.005~0.005	0.5
$d\Delta\beta$	k_{e2}	0.1~0.3	-0.002~0.002	0.2
$\Delta\theta_1$	k_{u1}	0.01~1	-0.12~0.12	0.02
$\Delta\beta_1$	k_{u2}	0.1~1.5	-0.1~0.1	0.1
θ_d	k_{e3}	0.8~1.1	-0.005~0.005	0.9
$d\theta_d$	k_{e3}	0.9~1.2	-0.001~0.001	1
β_d	k_{u3}	0.8~1.1	-0.005~0.005	0.9
$d\beta_d$	k_{e4}	0.9~1.2	-0.001~0.001	1
$\Delta\theta_2$	k_{e4}	0.5~1	-0.01~0.01	0.6
$\Delta\beta_2$	k_{u4}	0.5~1	-0.01~0.01	0.6

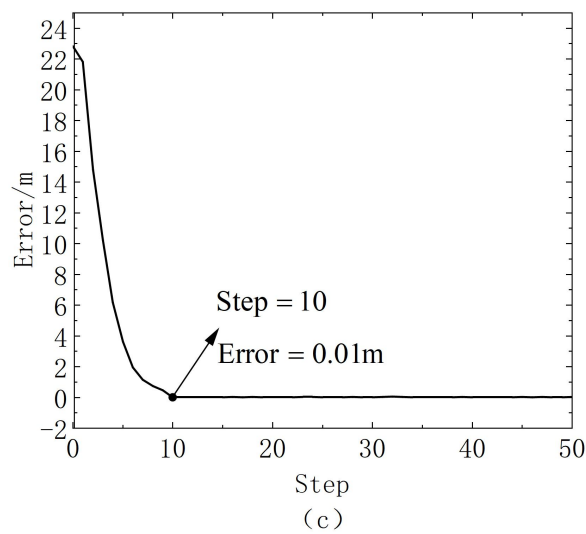
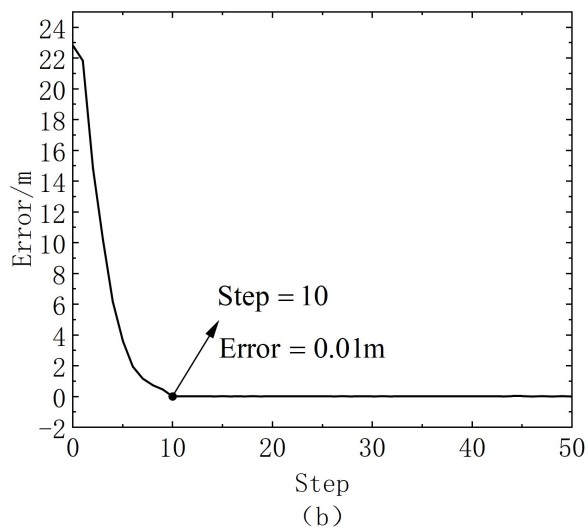
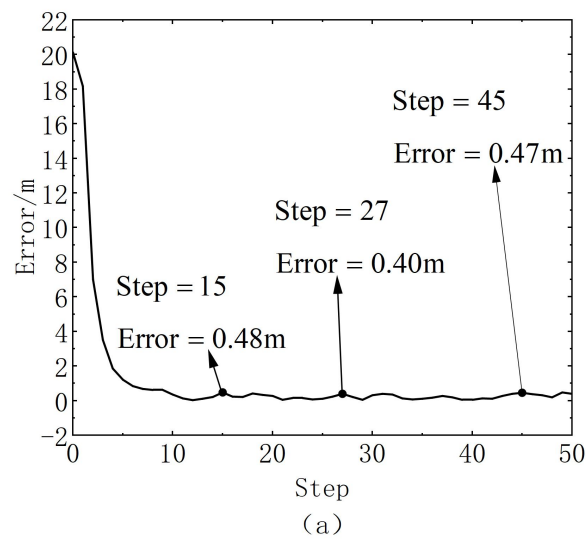


Figure 9. Drop point control error considering constant horizontal wind and ship motion disturbances: (a) based on nonadaptive fuzzy controller under actual ship motion disturbances; (b) based on double adaptive fuzzy controller under actual ship motion disturbances; (c) based on double adaptive fuzzy controller under predicted ship motion disturbances.

Table 9. Comparison of firefighting operation performance of different control methods ([6] and this paper).

Simulation Content	Response Time/Steps (Number of Simulation Steps)	RMSE/m (10 Steps to 50 Steps)
Nonadaptive fuzzy control (real disturbances)	$+\infty$	0.0675
Double adaptive fuzzy control (real disturbances)	10	3×10^{-3}
Double adaptive fuzzy control (predicted disturbances)	10	3×10^{-3}

Figure 9a shows the error of jet drop point control by a nonadaptive fuzzy controller with parameters set as in Table 5 under the disturbances of actual changes in ship motion attitudes. Figure 9b shows the error of drop point control by the double adaptive fuzzy controller with parameters shown in Table 8 in the case of actual disturbances. Figure 9c shows the error of drop point control by the double adaptive fuzzy controller with parameters shown in Table 8 in the case of predicted disturbances. Figure 9a shows that steady-state errors occur in actual offshore firefighting operations due to ship motion disturbances. In the current operating environment, a maximum drop point error of nearly 50 cm can be generated. The higher the sea state level is, the larger the error is, which seriously affects operational accuracy and efficiency. As shown in Figure 9b,c, the RMSE of the simulation results of the double adaptive fuzzy controller is only 3×10^{-3} m in the 10~50 steps simulation results, with fast response and high control accuracy.

6. Conclusions

In this paper, a control method for water cannons of unmanned fireboats considering wind and ship motion disturbances is presented. A prediction model of water cannon jet trajectory considering the constant horizontal wind was established, and the effective range of a water cannon’s angles was obtained. An online PSO was introduced to realize the controller’s self-adjusting parameters to adapt to environmental factors change, which makes up for the shortcomings of sensitivity and poor adaptability of fuzzy control parameters. By fusing visual recognition information and predicted ship motion attitudes information, a double adaptive fuzzy controller was designed to effectively resist the disturbance caused by wind and ship motion attitudes. At last, this control method was experimentally verified. The results show that the adaptive fuzzy controller can adapt to the changes in environmental factors by self-adjusting parameters. It takes only 0.6 s to make the drop point error less than 5×10^{-2} m and enter a stable and effective state. Compared with the traditional fuzzy control, the efficiency was improved by about 20%~50%. Meanwhile, based on the actual or predicted attitudes data, the dual adaptive fuzzy control can enter a stable and effective state at ten simulation steps. Moreover, the RMSE of the fall point error of the simulation between 10 and 50 steps was only 3×10^{-3} m, which can effectively resist disturbances and improve the operation efficiency and accuracy. As a result, the control effect of the method is remarkable and provides a theoretical reference and practical basis for future unmanned and intelligent research of marine firefighting technology. Furthermore, due to the limited step size of fuzzy control, frequent adjustment of the attitude of the water cannon may lead to excessive energy consumption and damage the service life of the equipment. Therefore, the next stage of research will be to design a controller based on an intelligent optimization algorithm and consider the driving frequency, again improving the performance of the control method.

Author Contributions: D.G.: conceptualization, methodology, validation, review and editing; W.X.: conceptualization, resources, methodology, validation, formal analysis, writing—review and editing; C.B.: funding acquisition; B.L.: formal analysis, data curation, validation, review and editing, supervision; J.Z.: funding acquisition. All authors have read and agreed to the published version of the manuscript.

Funding: The study was funded by the Shanghai Science and Technology Project of China (Grant 21DZ1205803, No.20040501200).

Institutional Review Board Statement: Not applicable.

Informed Consent Statement: Not applicable.

Data Availability Statement: Not applicable.

Conflicts of Interest: The authors declare no conflicts of interest.

References

1. Sanchi Collision: The Hull Burned Violently and the Oil Spill Area Increased Significantly. Available online: <https://baijiahao.baidu.com/s?id=1589446894872947351&wfr=s2pider&for=pc> (accessed on 13 January 2018).
2. Zhejiang Huahong 18 Flash Explosion in Wuhu Yangtze River Section, Killing 3 People. Available online: <http://finance.sina.com.cn/jjxw/2021-09-26/doc-iktzqtyt8231681.shtml> (accessed on 26 September 2021).
3. Zhu, J.; Li, W.; Lin, D.; Ge, Z. Study on water jet trajectory model of fire monitor based on simulation and experiment. *Fire Technol.* **2018**, *55*, 773–787. [[CrossRef](#)]
4. Wang, C.; Yuan, X.M.; Yang, Z.G.; Meng, Z.L.; Sun, J. Study on theoretical model of fire water monitor jet trajectory. *J. Yanshan Univ.* **2020**, *44*, 442–449. [[CrossRef](#)]
5. Li, W.H. Simulation of fire water jet trajectory based on simulink. In Proceedings of the 8th International Conference on Modern Mechanics, Ulan-Ude, Russia, 4 September 2022; pp. 449–453. [[CrossRef](#)]
6. Bian, Y.M.; Zeng, J.B.; Meng, M.; Li, M.R. Fire monitor water jet impact control based on fuzzy strategy. *Mechatronics* **2020**, *26*, 11–17. [[CrossRef](#)]
7. Zhu, J.; Li, W.; Lin, D.; Hengyu, C.; Ge, Z. Intelligent fire monitor for fire robot based on infrared image feedback control. *Fire Technol.* **2020**, *56*, 2089–2109. [[CrossRef](#)]
8. Liu, J. The jet closed-Loop control method based on image processing. In Proceedings of the 2021 IEEE International Conference on Progress in Informatics and Computing (PIC), Shanghai, China, 17–19 December 2021; pp. 179–183. [[CrossRef](#)]
9. Serrano, C.; Sierra-Garcia, J.E.; Santos Peñas, M. Hybrid optimized fuzzy pitch controller of a floating wind turbine with fatigue analysis. *J. Mar. Sci. Eng.* **2022**, *10*, 1769. [[CrossRef](#)]
10. Pham, D.A.; Han, S.H. Design of combined neural network and fuzzy logic controller for marine rescue drone trajectory-tracking. *J. Mar. Sci. Eng.* **2022**, *10*, 1716. [[CrossRef](#)]
11. Segura, E.; Vergara, E.; Rodríguez Melquiades, J.A.; Jiménez Carrión, M.; Sabino, C.; Gutiérrez Segura, F. A fuzzy optimization model for the berth allocation problem and quay crane allocation problem (BAP + QCAP) with n quays. *J. Mar. Sci. Eng.* **2021**, *9*, 152. [[CrossRef](#)]
12. Zheng, Z.; Wang, N. Adaptive frequency tracking control with fuzzy PI compound controller for magnetically coupled resonant wireless power transfer. *Int. J. Fuzzy Syst.* **2020**, *23*, 1890–1903. [[CrossRef](#)]
13. Li, Y.; Yu, J.; Guo, X.; Sun, J. Path tracking method of unmanned agricultural vehicle based on compound fuzzy control. In Proceedings of the 2020 IEEE 9th Joint International Information Technology and Artificial Intelligence Conference (ITAIC), Chongqing, China, 11–13 December 2020; pp. 1301–1305. [[CrossRef](#)]
14. Meng, J.; Wang, Z.; Xu, R.; Li, D. Research on active suspension control of high-speed train based on fuzzy compound strategy. *J. Syst. Simul.* **2021**, *33*, 1554. [[CrossRef](#)]
15. Sepehrzad, R.; Moridi, A.; Hassanzadeh, M.E.; Seifi, A.R. Intelligent energy management and multi-objective power distribution control in hybrid micro-grids based on the advanced fuzzy-PSO method. *ISA Trans.* **2020**, *112*, 199–213. [[CrossRef](#)] [[PubMed](#)]
16. Aghda, S.; Mirfakhraei, M. Improved routing in dynamic environments with moving obstacles using a hybrid fuzzy-genetic algorithm. *Future Gener. Comput. Syst.* **2020**, *112*, 250–257. [[CrossRef](#)]
17. Achom, A.; Das, R.; Pakray, D.P. An improved fuzzy based GWO algorithm for predicting the potential host receptor of COVID-19 infection. *Comput. Biol. Med.* **2022**, *151*, 106050. [[CrossRef](#)] [[PubMed](#)]
18. Essa, M.; Aboeela, M.; Moustafa Hassan, M. Position control of hydraulic servo system using proportional-integral-derivative controller tuned by some evolutionary techniques. *J. Vib. Control* **2014**, *22*. [[CrossRef](#)]
19. Zheng, K.; Zhang, Q.; Youmin, H.; Wu, B. Design of fuzzy system-fuzzy neural network-backstepping control for complex robot system. *Inf. Sci.* **2021**, *546*, 1230–1255. [[CrossRef](#)]
20. Pamucar, D.; Božanić, D.; Puška, A.; Marinkovic, D. Application of neuro-fuzzy system for predicting the success of a company in public procurement. *Decis. Making Appl. Manag. Eng.* **2022**, *5*, 2620–0104. [[CrossRef](#)]

21. Gharib, M. Comparison of robust optimal QFT controller with TFC and MFC controller in a multi-input multi-output system. *Rep. Mech. Eng.* **2020**, *1*, 151–161. [[CrossRef](#)]
22. Xu, D.; Cen, H. A hybrid energy storage strategy based on multivariable fuzzy coordinated control of photovoltaic grid-connected power fluctuations. *IET Renew. Power Gener.* **2021**, *15*, 1826–1835. [[CrossRef](#)]
23. Li, W.; Wang, G.G.; Gandomi, A. A survey of learning-based intelligent optimization algorithms. *Arch. Comput. Methods Eng.* **2021**, *28*, 3781–3799. [[CrossRef](#)]
24. Anderson, J. *Fundamentals of Aerodynamics*; McGraw Hill: New York, NY, USA, 2006; pp. 207–210.
25. Pu, F.; Rui, Y. *External Ballistics*; National Defense Industry Press: Beijing, China, 1989; pp. 21–23.
26. Jin, Z.; ShuYun, W. Selection of fuzzy subsets in fuzzy-controlled AC speed control systems. *Micro-Motor* **2003**, *36*, 31–35. [[CrossRef](#)]
27. Tang, Z.; Sun, Q.; Li, Y.; Song, M. Ship motion attitude prediction based on empirical mode decomposition and gaussian process regression. In Proceedings of the 2021 IEEE 4th International Conference on Electronic Information and Communication Technology (ICEICT), Xi'an, China, 18–20 August 2021; pp. 689–694. [[CrossRef](#)]

Disclaimer/Publisher's Note: The statements, opinions and data contained in all publications are solely those of the individual author(s) and contributor(s) and not of MDPI and/or the editor(s). MDPI and/or the editor(s) disclaim responsibility for any injury to people or property resulting from any ideas, methods, instructions or products referred to in the content.